J Soils Sediments (2009) 9:194–205
DOI 10.1007/s11368-009-0082-0

SOILS, SEC 1 • SOIL ORGANIC MATTER DYNAMICS & NUTRIENT CYCLING • RESEARCH ARTICLE

Biogenic calcium phosphate transformation in soils over millennial time scales

Shinjiro Sato · Eduardo G. Neves · Dawit Solomon · Biqing Liang · Johannes Lehmann

Received: 27 August 2008 / Accepted: 6 March 2009 / Published online: 9 April 2009

Abstract
Background, aim, and scope Changes in bioavailability of phosphorus (P) during pedogenesis and ecosystem development have been shown for geogenic calcium phosphate (Ca-P). However, very little is known about long-term changes of biogenic Ca-P in soil.
Materials and methods Long-term transformation characteristics of biogenic Ca-P were examined using anthropogenic soils along a chronosequence from centennial to millennial time scales.
Results and discussion Phosphorus fractionation of Anthrosols resulted in overall consistency with the Walker and Syers model of geogenic Ca-P transformation during pedogenesis. The biogenic Ca-P (e.g., animal and fish bones) disappeared to 3% of total P within the first ca. 2,000 years of soil development. This change concurred with increases in P adsorbed on metal-oxides surfaces, organic P, and occluded P at different pedogenic time. Phosphorus K-edge X-ray absorption near-edge structure (XANES) spectroscopy revealed that the crystalline and therefore thermodynamically most stable biogenic Ca-P was transformed into more soluble forms of Ca-P over time. While crystalline hydroxyapatite (34% of total P) dominated Ca-P species after about 600–1,000 years, β-tricalcium phosphate increased to 16% of total P after 900–1,100 years, after which both Ca-P species disappeared. Iron-associated P was observable concurrently with Ca-P disappearance. Soluble P and organic P determined by XANES maintained relatively constant (58–65%) across the time scale studied.
Conclusions Disappearance of crystalline biogenic Ca-P on a time scale of a few thousand years appears to be ten times faster than that of geogenic Ca-P.

Keywords Adsorption · Amazonian Dark Earths · Anthrosols · Dissolution · Organic phosphorus · Oxisols · Phosphorus transformation · Speciation · *Terra Preta de Índio* · XANES (X-ray absorption near-edge structure)

Responsible editor: Chengrong Chen

S. Sato · D. Solomon · B. Liang · J. Lehmann (✉)
Department of Crop and Soil Sciences, Cornell University,
Bradfield Hall,
Ithaca, NY 14853, USA
e-mail: CL273@cornell.edu

E. G. Neves
Museu de Arqueologia e Etnologia, Universidade de São Paulo,
Av. Prof. Almeida Prado, 1466, Cidade Universitária, Butantã,
São Paulo, SP 05508-070, Brazil

Present Address:
S. Sato
Southwest Florida Research and Education Center,
University of Florida,
2686 State Road 29 North,
Immokalee, FL 34142, USA

1 Background, aim, and scope

Phosphorus (P) is one of the most limiting nutrients to plants grown in soils worldwide, especially in highly weathered, acid soils in the tropics (Vitousek and Sanford 1986). Not only is P a minor constituent in soils as phosphate minerals (Lindsay et al. 1989), but also the biological availability of P is extremely limited when P is naturally or deliberately introduced to the soil system (Holford 1997). The soil P cycles that affect its bioavailability include dissolution–precipitation (mineral equilibrium), sorption–desorption (equilibrium between soil solution and solid phases), and mineralization–immobilization (transformations of P between inorganic and organic forms; Sims and Pierzynski

2005). Moreover, different soil reactions play important roles in determining P bioavailability during different stages of pedogenesis (Walker and Syers 1976; Tiessen et al. 1984).

Chronological influences on soil's physical, chemical, and morphological changes during pedogenesis vary depending on geology, geography, and ecosystem in which soils develop (Stevens and Walker 1970). Yet, several trends have been generally identified during soil development, which include pH decline, organic matter accumulation, carbonate loss, basic cation removal, clay formation, and clay mineralogical transformation. Walker and Syers (1976) introduced a conceptual model of soil development and its ecological implications by analyzing transformations in soil P, vegetation, and other ecosystem properties during pedogenesis, based on studies involving a range of soil sequences (0 to 130,000 years) in New Zealand. The validity of this model has been confirmed for the most part for Hawaiian soils from six different sites ranging in age from 300 to 4.1 million years (Crews et al. 1995) and in a group of 168 soil samples from all regions of the US representing eight soil orders of the Soil Taxonomy in different pedogenesis phases (Tiessen et al. 1984). According to the Walker and Syers model and others (Tiessen and Stewart 1985), the initial form of soil P is that of primary minerals (predominantly calcium phosphate, Ca-P as apatite minerals) at the beginning of soil development. During weathering of the primary and secondary minerals, metal ions such as aluminum (Al^{3+}) and iron (Fe^{3+}) are released from the minerals, then Al- and Fe-oxyhydroxides are formed. Dissolved inorganic P (P_i) is adsorbed to the metal-oxyhydroxide surfaces to form Al- and Fe-phosphate (Al-P and Fe-P) compounds. Adsorbed P_i can desorb in response to plant uptake of solution P or in exchange with other anions in solution or exuded from roots. Over long periods of time, P will become more occluded by Al- and Fe-oxyhydroxides during soil development. Phosphorus desorbed from the metal-oxides surfaces and/or dissolved from the mineral compounds is also taken up by soil organisms, thus transforming into organic P (P_o), but may be cycled back to the inorganic pool by mineralization of P_o (Crews et al. 1995).

However, in addition to this geogenic Ca-P, soils and sediments may also contain or be enriched with biogenic sources of P (Pattan et al. 1995; Lima et al. 2002; Lehmann et al. 2004; Tarawneh and Moumani 2006). Amazonian Dark Earths (ADEs; i.e., Anthrosols, locally known as *Terra Preta de Índio*), patchily distributed throughout the Amazon Basin in Brazil, were found to contain microfragments of biogenic apatite in the form of animal bone and fish spine particles of varying morphologies, which were attributed to high P and Ca contents in soils (Lima et al. 2002; Schaefer et al. 2004). The main biogenic components in sedimentary phosphorite concretions found in Umm Rijam Chert Limestone Formation in the Ma'an area, southern Jordan were fragments of macrofossils (bivalves) and microfossils (planktonic foraminifera) in different proportions (Tarawneh and Moumani 2006). Chemical analyses of surface sediments in the Wharton Basin in the Indian Ocean suggested accumulation of biogenic apatite (fish bone debris) from high biological productivity waters (Pattan et al. 1995). While the long-term dynamics of geogenic Ca-P are relatively well quantified (Walker and Syers 1976; Crews et al. 1995; Vitousek and Farrington 1997; Hedin et al. 2003), limited information is available on the time required for transformation of biogenic Ca-P. Since biogenic Ca-P structurally differs from geogenic Ca-P (Rao et al. 2000; Tang et al., 2003a), different dynamics can be expected.

This study has, as objectives, to determine the transformation characteristics of biogenic Ca-P over a long period of time stretching from centennial to millennial time scales and to compare the transformation dynamics between biogenic Ca-P from this study and geogenic Ca-P as modeled by Walker and Syers (1976).

2 Materials and methods

2.1 Site and soil descriptions and soil analyses

Soil material was collected from four different archaeological sites near Manaus, Brazil (3°8' S, 59°52' W, 40–50 m above sea level): Hatahara (HAT), Lago Grande (LG), Açutuba (ACU), and Dona Stella (DS). The mean annual precipitation is about 2,088 mm with the maximum between December and May (204–298 mm per month, 73% of annual rainfall), air temperature of 26.6°C, and atmospheric humidity of around 84% (Vose et al. 1992). The natural vegetation is a tropical lowland rainforest. The studied soils were Anthrosols (Kern et al. 2003) and their adjacent soils developed on Oxisols and Spodosols (USDA 1999). Among many different additions, these Anthrosols also received large amounts of biogenic Ca-P in form of fish bones (Lima et al. 2002; Lehmann et al. 2004; Schaefer et al. 2004). The selected sites were occupied at different times in the past (Table 1, modified from Neves et al. 2003, EG Neves, unpublished data), which allowed the investigation of effects of pedogenic time on P species and transformation of biogenic Ca-P. Samples were taken from the entire soil profile according to genetic horizons, mostly (except for LG) from subsurface horizons below a layer of potsherds to exclude recent anthropogenic additions. Samples from adjacent soils were taken from the A horizon at locations approximately double the distance from sites for counterpart Anthrosols with maximum color difference to ensure minimal anthropogenic effects. All samples were air-dried and large plant debris was removed. In addition, A horizon soil samples

Table 1 Selected properties of selected horizons from the studied Anthrosols and adjacent soils in the central Amazon

Site	Type	Depth cm	Age year	Sand %	Silt	Clay	pH[a]	Organic C g kg^{-1}	Total N	Total P mg kg^{-1}	Total Ca	Total Al	Total Fe	Total cations[b]	CEC[c] cmol$_c$ kg^{-1}	C/N	C/P$_o$	N/P$_o$
Hatahara	Anthrosol	43–69	600–1,000	51.3	21.7	27.0	6.4	22.0	1.0	9,064	17,545	53,696	29,399	104,661	21.1	22	54	2
	Adj. soil	0–10		60.4	3.8	35.9	4.6	21.8	1.6	273	115	58,552	30,246	89,243	8.8	14	357	26
Lago Grande	Anthrosol	0–16	900–1,100	47.9	29.6	22.6	5.9	31.5	1.8	5,026	6,354	64,010	47,097	119,002	22.2	18	74	4
	Adj. soil	0–8		69.4	3.9	26.7	4.2	17.5	1.3	251	119	45,094	44,409	90,011	5.9	13	471	35
Açutuba	Anthrosol	48–83	2,000–2,300	81.9	7.7	10.4	5.6	15.7	1.0	777	332	24,357	21,677	46,754	5.6	16	115	7
	Adj. soil	0–30		87.9	3.6	8.5	4.7	15.4	0.8	198	50	16,624	16,044	32,817	5.2	19	361	19
Dona Stella	Anthrosol	190–210	6,700–8,700	96.8	2.9	0.3	5.0	16.5	1.1	139	40	1,989	1,766	3,834	2.7	15	439	29
	Adj. soil	0–12		91.1	8.6	0.3	3.9	10.2	0.4	51	165	1,043	708	1,987	8.1	26	1,219	48

P$_o$ total organic P fraction as sum of bicarbonate-P$_o$ and hydroxide-P$_o$ in the P fractionation results (Table 2).

[a] 1:2.5 H_2O

[b] Sum of total elemental Ca, Mg, K, Na, Al, and Fe

[c] Potential cation exchange capacity

(Oxisols) from a primary forest site in the central Amazon with the minimum or no anthropogenic influences were used for comparison purpose with the Anthrosols (Lehmann et al. 2001). Selected properties of the forest soil were: pH4.1, 21.4% sand, 59.0% clay, 40.6 g kg^{-1} total organic carbon (C), 4.2 mg kg^{-1} Mehlich-3 extractable P, and 220 mg kg^{-1} total P (Lehmann et al. 2004).

Soil samples from each site were sieved to 2 mm, homogenized, and finely ground for combustion analyses. Organic C and total nitrogen (N) were determined using a Europa ANCA GSL sample combustion unit (PDZEuropa, Crewe, England). Soil pH was determined in 1:2.5 soil/water ratio using a SP20 glass electrode (Thermo Orion, Cambridge, MA, USA). Soil texture was determined using the pipette method (Gee and Or 2002). Total elemental P, Ca, magnesium (Mg), potassium (K), sodium (Na), Al, and Fe were determined according to procedure EPA 3052 (USEPA 1995) using nitric and hydrofluoric acid, and quantified by inductively coupled plasma atomic emission spectrometry (ICP-AES, Spectro CIROS, CCD, Germany). Soil potential cation exchange capacity (CEC) was determined with ammonium acetate (1 M, 2.5 g soil, total of 25 mL) at pH7.0 using soil samples with and without peroxide digestion to remove non-black carbon (BC). Twenty grams of soil were treated with 30% (*w*/*w*) peroxide (initially 10 mL with daily additions up to a total of 30–35 mL until no further bubbles appeared) and heated on a hot plate at 90°C to ensure maximum non-BC removal.

2.2 Phosphorus sequential fractionation

Phosphorus fractions were determined by a sequential extraction following a modified procedure of Tiessen and Moir (1993). A half gram of soil was weighed into a 50-mL centrifuge tube, then 25 mL of deionized water and two strips of anion-exchange resin (1×6 cm; Ionac MA-7500, Sybron Chemicals, Birmingham, NJ, USA) were added to the tubes. The tubes were shaken for 16 h on a horizontal shaker. After the resin strips were removed, the tubes were centrifuged for 20 min at 0°C at 25,000×*g*, and water was discarded. The resin strips were placed in a clean 50-mL tube with 20 mL of 0.5 M HCl, and shaken for 16 h. Inorganic P in the 0.5 M HCl solution was determined as described below. Then, 25 mL of 0.5 M $NaHCO_3$ (pH8.5) was added to each tube (by weight), vortexed, shaken for 16 h, and centrifuged as above. The supernatant was filtered through a 0.45-μm filter (Millipore, Billerica, MA, USA). Inorganic and total P (P$_t$) in the bicarbonate extract were determined as below. The extraction process was repeated using 25 mL of 0.1 M NaOH and 1 M HCl as above; and P$_i$ and P$_t$ in the hydroxide extract, and P$_i$ in the dilute acid extract were determined as below. Then, the soil residue was heated with 10 mL of concentrated HCl in a

water bath at 80°C for 20 min. After being removed from the hot bath, a further 5 mL of concentrated HCl was added to each tube, vortexed, and allowed to stand at room temperature for 1 h. The tubes were centrifuged and filtered into a 50-mL volumetric flask. Ten milliliters of deionized water was added to each tube to wash the soil residue, vortexed, centrifuged as above, and decanted into a flask twice. The flask was made up to the volume with deionized water and P_i and P_t in the HCl solution were determined. Then, soil residue was transferred into a 75-mL digestion tube using deionized water, then 5 mL of concentrated H_2SO_4 was added, and digested on a heating block at 360° C by treating the solution with hydrogen peroxide following the method of Thomas et al. (1967). The digested solution was filtered and P_i in solution was determined.

Inorganic P, as soluble reactive P, was determined by the method of Murphy and Riley (1962) on a spectrophotometer at 880 nm. The bicarbonate and hydroxide extracts were acidified by adding 0.9 M H_2SO_4 to precipitate organic matter prior to P_i determination as above. Total P was digested by adding ammonium persulfate and 0.9 M H_2SO_4 following USEPA method 365.1 (USEPA 1983). Organic P in the bicarbonate and hydroxide extracts was determined as the difference between P_t and P_i in the respective extract.

The interpretation of P in each extract is based on an understanding of the action of individual extractants, their sequence, and their relationship to the chemical and biological properties of the soil (Tiessen and Moir 1993). Resin-P is reasonably well-defined as freely exchangeable and bioavailable P_i. The bicarbonate-extract presumably removes labile P_i and P_o sorbed on soil minerals and a small amount of microbial P. The hydroxide-P would represent Al- and Fe-associated P_i and P_o that are strongly held to soil surfaces by chemisorption. The dilute acid-P_i is clearly defined as Ca-bound P_i, and there is rarely any P_o in this extract. The concentrated acid extract is useful for distinguishing P_i and P_o in very stable residual pools. The acid-digested P is unlikely to contain anything but highly recalcitrant P_i (Cross and Schlesinger 1995).

2.3 X-ray absorption near-edge structure spectroscopy analysis

Solid-state characterization of P from the soil, P standards, and fish bones was carried out using P K-edge X-ray absorption near-edge structure (XANES) spectroscopy at beamline X-19A of the National Synchrotron Light Source at Brookhaven National Laboratory. The P-XANES spectra were collected from air-dried silt and clay fractions (by dry sieving to <50 μm) of soil samples and P standards and fish bones that had been passed through a 125-μm sieve prior to analysis. The finely ground materials were uniformly spread on Scotch tape, which was pre-tested for its P level and exhibited a much lower P level than the amount detected from Mylar X-ray film (commonly used for covering samples; Complex Industries, New York, USA) and mounted at the back of a center-through hollow (1.3 cm diameter) 0.5-mm thick acrylic sample holder. The measurements were conducted under standard operating conditions; i.e., after calibrating the X-ray energy to the K-edge of P using variscite (VAR) as a standard, the spectrum was assigned a reference energy (E_0) value of 2,149 eV and scans ranging from 40 eV below to 100 eV above the absorption edge of P. Technical limitations of the beamline prohibited going further below the P K-edge, which may make background subtraction in the case of more dilute samples a challenge (Peak et al. 2002). Low total P concentrations in the material, as seen in some of soil samples studied particularly from adjacent sites, can result in spectra with low quality and high noise. For these reasons, the materials were not diluted in boron nitride (BN_3). The XANES data were collected with varying step sizes (0.5 eV during 2,109–2,139 eV, 0.08 eV 2,139–2,155 eV, 0.2 eV 2,155–2,179 eV, and 1.0 eV 2,179–2,249 eV). Each XANES spectrum was composed of an average of three scans. A monochromator consisting of double crystal Si (III) with an entrance slit of 0.5 mm, electron beam energy of 2.5 GeV and maximum beam current of 300 mA was used. The spectra were recorded in fluorescence mode using a passivated implanted planar silicon (PIPS) detector (Canberra Industries, Meriden, CT, USA). The beam path from the incident ion chamber to the sample chamber was purged with He gas. The P-XANES data analysis was done using WinXas version 3.1 (WinXas Software, Hamburg, Germany). The energy scale was calibrated to E_0 of 2,149 eV as the maximum energy of the first peak in the first derivative spectrum for VAR standard. The background was corrected by fitting a first-order polynomial to the pre-edge region from 2,119 to 2,139 eV and the spectra were normalized over the reference energy of 2,149 eV.

Linear combination fitting (LCF) analysis of P-XANES spectra for the soil samples was conducted over the spectral region from 2,142 to 2,162 eV using Kaleidagraph (version 3.6, Synergy Software, Reading, PA, USA; Hutchison et al. 2001). This spectral region was selected because the LCF analysis using the whole spectral range was difficult to obtain reliable results particularly from soil samples with low P concentrations, and it covers all of the spectral features for P species of interest for our study (Sato et al. 2005). The following materials were used as P standards for comparison with the sample spectra (Sato et al. 2005): fish bones, dibasic calcium phosphate (DCP), dibasic calcium phosphate dehydrate (DCPD), β-tricalcium phosphate (TCP), amorphous calcium phosphate phase 1 (ACP1),

octacalcium phosphate (OCP), synthesized hydroxyapatite (HAP), strengite (STR), VAR, and such aqueous orthophosphate species as $H_2PO_4^-$ (Aq-PO_4). All possible ternary combinations of the ten available standards were fitted without energy shift parameters and the best fitting results were judged according to their chi-square values. The fitting results were rejected when at least one of the best fit coefficients for the standard spectra were negative. Quantitatively distinguishing P-XANES spectra between Aq-PO_4, very weakly bound P associated with organic matter, and P_o (e.g., aqueous phytic acid) is very difficult lacking distinctive spectral features (Peak et al. 2002), therefore Aq-PO_4 in the LCF results may indicate a combination of soluble P and P_o, since no P_o species were measured in XANES analysis in our study. Furthermore, a spectral feature indicative of the presence of Fe-associated P in the material increases in intensity with increasing mineral crystallinity (e.g., P adsorbed on ferrihydrite<P adsorbed on goethite<non-crystalline Fe-P<crystalline Fe-P, STR; Beauchemin et al. 2003). Since none of the Fe-associated P other than STR were used for the LCF analysis in our study, it is possible that the LCF analysis results as STR, although the peak is small, which may in fact indicate the presence of P adsorbed on Fe-oxyhydroxides.

2.4 Statistical analyses

Linear regressions and *t* tests were performed using STATISTICA 6 (StatSoft, Tulsa, OK, USA).

3 Results

3.1 Soil properties

The pH values were significantly greater in Anthrosols than adjacent soils with averages of 5.7 and 4.4, respectively (p= 0.007, Table 1). To eliminate inherent differences among sites, total P, and total Ca contents in adjacent soils were subtracted from respective contents in the Anthrosols for each site, then the adjusted total P and total Ca contents exponentially decreased over time (Fig. 1). Proportions of total Ca in the total cations (sum of total elemental Ca, Mg, K, Na, Al, and Fe) in Anthrosols, after subtracting those in adjacent soils for each site, steadily decreased over time from 113% to 22%, 2%, and –7% for HAT, LG, ACU, and DS, respectively. On the other hand, the proportions of the sum of total Al and Fe in the total cations in Anthrosols progressively increased over time from –37% to 75%, 96%, and 108% for the sites listed above. Potential CEC was distinctly higher only in HAT and LG Anthrosols than those in any other soils. Organic C in Anthrosols was slightly higher in some sites (1–2% in HAT and ACU) and

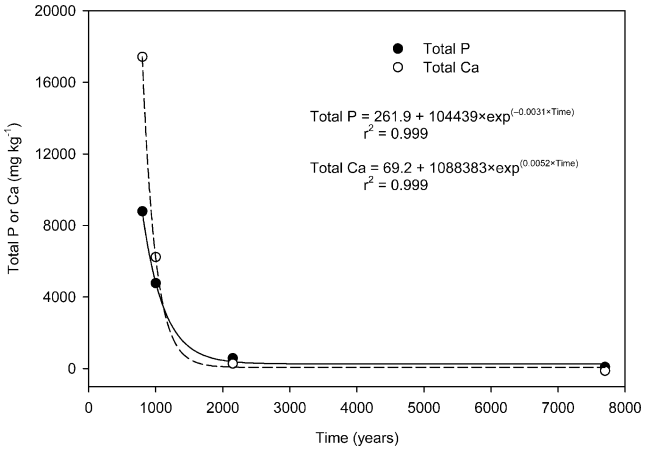

Fig. 1 Total phosphorus (P) and total calcium (Ca) in the studied Anthrosols as a function of time. Total P and total Ca contents in adjacent soils are subtracted from respective contents in Anthrosols for each site. Time is the average of age range of each Anthrosol

greatly higher in other sites (62–80% in DS and LG) compared with that in respective adjacent soil, but there was no effect of time found on organic C in Anthrosols. Total N was not necessarily higher in Anthrosols compared to adjacent soils and no significant trend was found in total N in Anthrosols relative to site ages. The C/N ratio slightly decreased over time in Anthrosols from 22 to 15, while those of ACU and DS adjacent soil were slightly higher than those of HAT and LG. Both C/P_o and N/P_o ratios (total P_o fractions as sum of bicarbonate-P_o and hydroxide-P_o in the P fractionation results below) in Anthrosols continuously increased over time, reaching levels comparable with those in adjacent soils except for that in DS.

3.2 Phosphorus fractions

Changes of different P fractions in Anthrosols in the chronosequence are presented in the same format as presented by Walker and Syers (1976), as fractions of total P (Fig. 2, Table 2). It is assumed that all P was present as Ca-bound P_i at time zero when fish and animal bones would have been deposited to Anthrosols as one of the major sources of human debris (Schaefer et al. 2004). It is noted that soils already contained P before the anthropogenic deposition as shown by the total P values found in adjacent soils (51–273 mg kg^{-1}). However, the amounts present in soils were small compared to the Ca-P additions as total P in the HAT adjacent soil was only 3% of that found in the corresponding Anthrosol with an age of 600–1,000 years (see Table 1).

The fraction of freely exchangeable P_i (resin-P_i) to total P increased at the beginning of soil formation and steadily declined afterwards, but consisted only to 6–9% of total P at all ages. Labile P_i and P_i adsorbed on soil surfaces, especially on metal surfaces of Al- and Fe-oxides

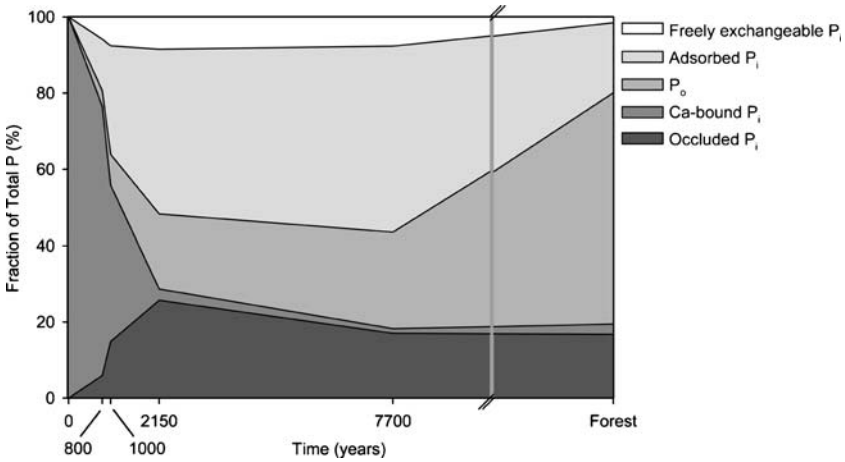

Fig. 2 Changes in phosphorus (P) fractions as percentage of total P in chronosequence in the studied Anthrosols. Phosphorus fractions of the background forest soils were taken from a primary forest with no signs of habitation from Lehmann et al. (2004). Freely exchangeable inorganic P (Pi)=resin-Pi, adsorbed Pi=bicarbonate-Pi+hydroxide-Pi, organic P (Po)=bicarbonate-Po+hydroxide-Po, calcium-bound Pi=dilute acid-P, and occluded Pi=concentrated acid- and acid-digested P

(bicarbonate-P_i and hydroxide-P_i, respectively) dramatically increased as a fraction of total P from the deposition of P until 2,150 years of soil formation (up to 43%), then showed a slow increase until 7,700 years (49%). These values were still greater than the values for adsorbed P_i found in uninfluenced forest soil (see Fig. 2). Organic P (sum of bicarbonate-P_o and hydroxide-P_o) continued to be small fractions of total P (4–8%) until 1,000 years, then increased to 20–25% by 7,700 years. In the forest soil, P_o was the major fraction of total P (61%). Calcium-bound P_i (dilute acid-P_i), deposited by human actions as animal residues, almost disappeared after the first 2,150 years of soil formation, then remained in small fractions (1–3%) at later stages. Highly stable and recalcitrant (occluded) P_i (sum of concentrated acid-P and acid-digested P) increased its proportion of total P up to 26% over time until 2,150 years and remained at 17% after 7,700 years.

Distribution of P in fractions of adjacent soils was remarkably different from that in the Anthrosols, and relatively similar among adjacent soils (Fig. 3). The majority of P was found in occluded P_i, ranging from 45% in DS to 70% in LG. On the other hand, Ca-bound P_i was almost non-existent in any of the adjacent soils (0.2–1.6%). Organic P was consistently present in all adjacent soils with 17–23% of total P. Small differences in fractions of adsorbed P_i and freely exchangeable P_i were observed among adjacent soils: 20%, 9%, 13%, and 13% adsorbed P_i, and 10%, 4%, 3%, and 20% freely exchangeable P_i of total P in HAT, LG, ACU, and DS soils, respectively.

3.3 Phosphorus species from XANES analyses

Nine standards of inorganic P species and fine bones were measured using XANES for comparison with spectra obtained from the investigated soils, but only those spectra for the P standards that are relevant for quantification analysis and for fish bones are shown (Fig. 4). The XANES spectra for the complete set of P standards investigated including spectral features and interpretation of chemical differences of P standard species are provided by Sato et al. (2005), therefore it is not presented here. A spectrum of fish bones closely resembled an overall shape of HAP spectrum except that a shoulder at 2,151–2,152 eV (Fig. 4 (c and d); hereafter spectral features are indicated by the figure

Table 2 Phosphorus (P) fractionation of the studied Anthrosols and adjacent soils (concentration in mg kg^{-1}±standard deviations)

Site	Type	Resin-P_i mg kg^{-1}	Bicarbonate-P_i	Bicarbonate-P_o	Hydroxide-P_i	Hydroxide-P_o	Dilute acid-P_i	Acid-P	Digested P
Hatahara	Anthrosol	578±44	335±47	309±56	1,001±105	100±11	6,994±25	485±13	99±5
	Adj. soil	30±22	8±2	18±0	48±19	43±8	4±3	83±9	55±1
Lago Grande	Anthrosol	397±11	219±1	228±19	1,275±92	198±53	2,141±67	584±0	193±10
	Adj. soil	9±1	3±0	6±2	17±0	31±1	0±0	73±33	85±1
Açutuba	Anthrosol	59±5	84±5	64±4	218±5	72±10	21±1	141±13	38±3
	Adj. soil	6±1	5±0	8±1	18±2	35±0	2±1	68±4	46±0
Dona Stella	Anthrosol	11±2	53±10	28±4	20±5	9±1	2±1	21±3	5±1
	Adj. soil	8±6	4±0	2±1	1±1	7±1	1±0	10±0	8±1

P_i inorganic P, *P_o* organic P

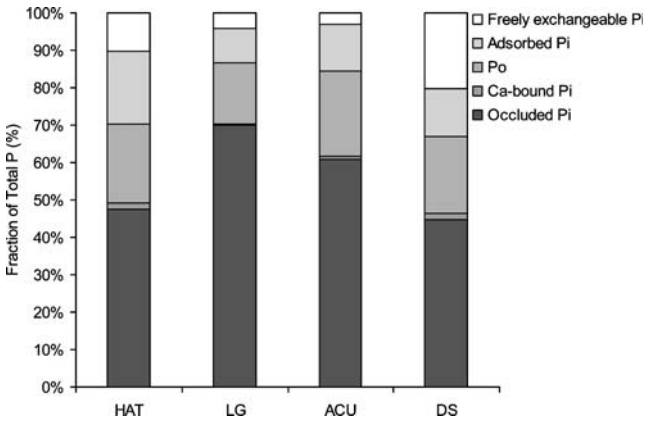

Fig. 3 Phosphorus (P) fractions as percentage of total P in adjacent soils. Definitions of P fractions follow those in Fig. 2. *HAT* Hatahara, *LG* Lago Grande, *ACU* Açutuba, *DS* Dona Stella

number and spectral feature letter) appeared slightly less pronounced than that of HAP but slightly better defined than that of OCP (OCP spectrum from Sato et al. 2005).

The heterogeneity of the soil samples, especially those with low total P, affects the quality of spectra and consequently presents a challenge for the interpretation of P-XANES spectra. However, several spectral features can be assigned to chemical P forms in spectra for Anthrosols and adjacent soils (Fig. 5). Beside the white line (4b) and oxygen oscillation (4f), the peak at 2,159 eV (5a (e)) and the shoulder at 2,151–2,152 eV (5a (c and d)) were seen in all Anthrosol spectra. Both spectral features indicate the presence of Ca-P species in those soils. It appears that the shoulder (5a (c and d)) was better defined in the following order: DS<ACU<LG<HAT, although a small feature which may be considered as spectral noise appeared towards the high energy end of the shoulder in the DS spectrum. In fact, the LCF analysis resulted in decreasing proportions of more stable Ca-P species and increasing proportions of more soluble species over time (Table 3). While the proportion of HAP (the most stable Ca-P, 34%) was found only in HAT (the youngest soil), the proportion of TCP (less stable than HAP) significantly increased from 5% in HAT to 16% in LG, then eventually disappeared in ACU and DS (the oldest soil). Also, 17% of ACP1 (even less stable than TCP) appeared in the oldest soil (DS). The pronounced peak at 2,146 eV (4a), indicative of the presence of STR, was not seen in any spectra from Anthrosols, although a broadened peak at around 2,146 eV appeared to be more pronounced in the order of HAT<LG<ACU<DS. While the proportion of STR by the LCF increased from 0% (HAT) to 27% (LG) and 34% (ACU) then decreased to 20% in DS, the proportion of Aq-PO_4 maintained relatively constant levels at 58–65% regardless of the soil age (Table 3).

Phosphorus-XANES spectra for adjacent soils, due to overall low total P concentrations, were not well-defined, showing many spectral noises, especially in ACU and DS, compared to those for Anthrosols (Fig. 5b). The pre-white line peak (5b (a)) indicative of Fe-P was identifiable in HAT and LG spectra, but not pronounced in ACU and DS spectra. It appears that the Ca-P-specific peak at 2,159 eV (5b (e)) was shown in HAT, LG, and ACU spectra, but it was shifted towards the high energy side and difficult to distinguish from spectral noise. However, it appears that the shoulder indicative of the presence of Ca-P species (5b (c and d)) was also detected in all spectra for adjacent soils. The shoulder seemed to be more distinctive in the order of HAT<LG<ACU<DS. A seemingly small peak at around 2,142 eV (in HAT and LG) could not be concluded as spectral noises caused by low total P concentrations or identifiable peak since none of the P standards investigated

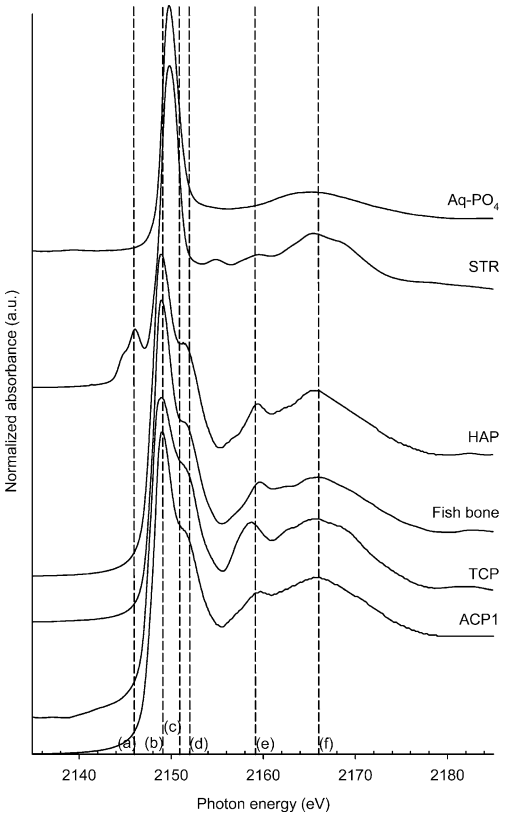

Fig. 4 Phosphorus (P) K-edge XANES spectra for selected inorganic P standard species and fish bone. Only those standard spectra relevant to quantification analysis are shown. The *dashed lines* show energy levels of importance to indicate unique spectral features for different P species: (*a*) strengite (STR), (*b*) absorption edge (*white line*); (*c*)–(*d*) calcium-P (Ca-P) species related to their solubility, (*e*) Ca-P, (*f*) oxygen oscillation. These spectra, including those of all other standard species studied, are a reproduction from Sato et al. (2005). *ACP1* amorphous calcium phosphate phase 1, *TCP* β-tricalcium phosphate, *HAP* hydroxyapatite, *Aq-PO_4* orthophosphate in aqueous solution (50 mM P in a 0.1 M NaCl background solution at pH4.7)

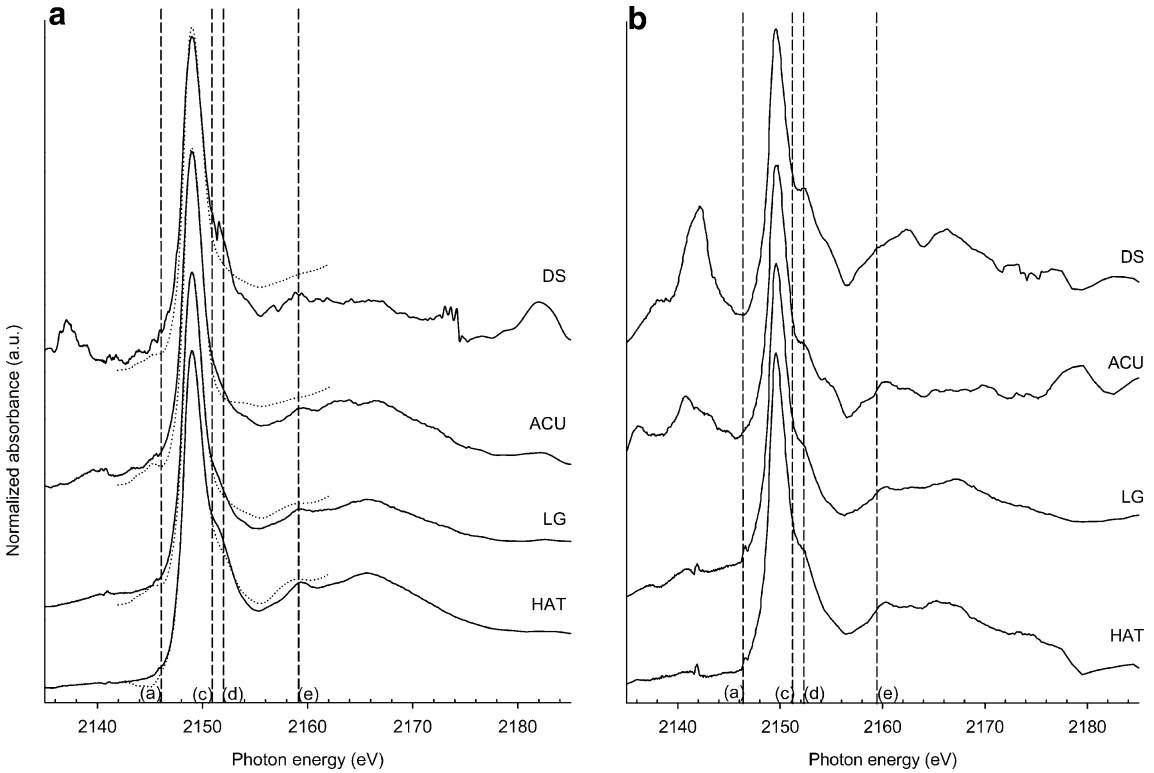

Fig. 5 Phosphorus (P) K-edge XANES spectra for Anthrosols (**a**) and adjacent soils (**b**). The *dashed lines* correspond to those in Fig. 4 and only those relevant to quantification analysis are shown. The *dotted lines* in (**a**) represent the best fitted result to respective spectra by linear combination fitting using an energy range of 2,142–2,162 eV

in our study could match the peak, although it appeared more widened in ACU spectrum and more pronounced in DS spectrum compared with those in HAT and LG. The LCF analysis was performed on spectra for adjacent soils; however, the accuracy of the analysis was questionable based on the chi-sq values and overall spectral noise so that the data were not presented here.

4 Discussion

Phosphorus is one of the key elements in soil development because of its ecological significance, and the soils are subject to strong weathering of primary P minerals (Walker and Syers 1976; Hedin et al. 2003). Total P derived from geogenic Ca-P across a four-million-year substrate age gradient of Hawaiian tropical forest soils showed a steep reduction between 2,000 and 20,000 years of pedogenesis as a result of weathering, as evidenced by the trend in silica (Si) loss during the same period of time (Hedin et al. 2003). For biogenic Ca-P in our study, over 90% of total losses of total P and total Ca occurred during the first ca. 2,000 years (see Fig. 1), which coincides with the rapid decrease of the Ca-bound P_i fraction from the P fractionation results (see Fig. 2). The LCF results of XANES spectra on Anthrosols suggest that the rapid decrease in Ca-P was endorsed by concurrent transformation of more stable Ca-P species to more soluble species with the decrease in the proportion of HAP in the youngest soil and the increase in the proportions of TCP and ACP1 in older soils within a few hundred years (see Table 3).

Rates of loss of Ca-P compounds in soil were shown to greatly vary among different ecosystems and climates. Over 99% of Ca-bound P in carbonates was lost within 500 years

Table 3 Relative proportions of phosphorus (P) standards that best fit the XANES spectra of the studied Anthrosols in linear combination fitting (percentage after normalization to sum=100%±standard errors for the linear coefficients)

Site	HAP %	TCP	ACP1	STR	Aq-PO_4	Chi-sq
Hatahara	34±5	5±4	0	0	61±1	0.091
Lago Grande	0	16±2	0	27±4	58±2	0.142
Açutuba	0	1±3	0	34±5	65±4	0.298
Dona Stella	0	0	17±4	20±7	63±5	0.601

HAP hydroxyapatite, *TCP* β-tricalcium phosphate, *ACP1* amorphous calcium phosphate phase 1, *STR* strengite, *Aq-PO_4* orthophosphate in aqueous solution (50 mM P in a 0.1 M NaCl background solution at pH4.7)

of soil development in dune sands on Vancouver Island, British Columbia (Singleton and Lavkulich 1987). In comparison, desert soils in The Jornada Basin, New Mexico still contained 54% Ca-bound P of its total P after more than 25,000 years (Lajtha and Schlesinger 1988). Furthermore, it has been shown that dissolution of sedimentary phosphate rocks (PRs; e.g., $Ca_{9.53}Na_{0.34}$ $Mg_{0.13}(PO_4)_{4.77}(CO_3)_{1.23}F_{2.49}$, from North Carolina, USA) is enhanced by soil properties such as low soil pH with high pH-buffering capacity, low Ca and P concentrations in soil solution, high soil P sorption capacity, high soil moisture content, and high organic matter content (Sale and Mokwunye 1993; Chien and Menon 1995). Therefore, highly weathered, acid soils of the humid tropical environment in the central Amazon may have accelerated dissolution and weathering rates of Ca-P in soil.

Dissolution rates of Ca-P compounds also depend on species, source, or crystal structure of the compound itself (Tang et al. 2003a). Comparing different phosphorites from western India, Rao et al. (2000) found that constituents and porosity of the initial substrate and physio-chemical conditions at the time of their formation were responsible for differences in macroscopic characteristics of phosphorites. The authors also found that a phosphorite that was formed involving fish excrement as the initial substrate was more friable and less dense than those involving parts of sediment, although both phosphorites contained apatite microparticles similar to fossilized microbes.

Tang et al. (2003b) listed the solubility activity product (K_{sp}) of several Ca-P species (e.g., DCPD, 2.32×10^{-7} mol^2 l^{-2}; TCP, 2.83×10^{-30} mol^5 l^{-5}; and OCP, 2.51×10^{-99} mol^{16} l^{-16}), and showed that the carbonated apatite (CAP; e.g., fish bones, PRs, and bone and dental hard tissues) had significantly greater K_{sp} than HAP (CAP, 2.88×10^{-112} mol^{18} l^{-18} and HAP, 5.52×10^{-118} mol^{18} l^{-18}). The authors also found that CAP dissolution rate was relatively insensitive to changes in Ca and P concentrations at higher undersaturations, suggesting the importance of the carbonate component under these conditions. The degree to which isomorphic substitution of phosphate by carbonate occurs within the apatite crystal structure is a key factor in determining the chemical reactivity of the apatite compound (Chien and Menon 1995). The XANES spectra in our study confirmed the relative solubility between CAP (or fish bones) and HAP based on how well-defined the shoulder at 2,151–2,152 eV was (indicative of Ca-P solubility; the better defined the shoulder, the more stable the Ca-P species; Sato et al. 2005). The order of definition of the shoulder for various Ca-P species also matches with their K_{sp} values listed above (DCPD<TCP<< OCP<CAP<HAP). This could explain relatively rapid dissolution and exhaustion of biogenic Ca-P in the studied Anthrosols (mostly derived from fish residues) compared with geogenic Ca-P in the Hawaiian soils (mostly derived from mineral phosphates; Crews et al. 1995), although the solubility of CAP and HAP appears almost indistinguishable (far smaller) compared with those of TCP and DCPD.

Changes in different P fractions over time as a result of dissolution of biogenic Ca-P were generally supported by the Walker and Syers (1976) model developed for geogenic Ca-P. According to the model, as Ca-bound P_i fraction declines during early soil formation, all other P fractions increase. Freely exchangeable and adsorbed P_i fractions (termed as non-occluded P_i in the model) increase at the beginning, but decline to minimum levels at approximately the same time as the Ca-bound P_i fraction disappears. On the other hand, occluded P_i increases and eventually predominates at later stages of soil development. Organic P also increases as Ca-P declines, then becomes one of the major fractions. While the dynamics were also observed for biogenic Ca-P in our study, an increase in occluded P_i and decreases in freely exchangeable and adsorbed P_i were not observed due to changes in texture and mineralogy between different ages of the Anthrosols studied (Liang et al. 2006), which were not related to the chronosequence, and therefore not tested with the soils studied here.

Soil weathering causes Al- and Fe-oxyhydroxides to be formed as bases and Si are lost from the system, allowing the formation of secondary Al- and Fe-P (Hsu 1977). As described by Walker and Syers (1976), most of the P released from biogenic Ca-P in our study was adsorbed on soil surfaces, especially on the metal surfaces of Al- and Fe-oxyhydroxides. This transformation was well-illustrated by the P fractionation with continued increase in the adsorbed P_i fraction over time (see Fig. 2). Furthermore, significant decreases in Ca-P namely HAP and concurrently significant increases in STR proportion over time (except for DS soil) seen in the LCF results of XANES spectra indicate the transformation of P from Ca-P species into Al- and Fe-associated P which may have included P adsorbed on the metal surfaces of Al- and Fe-oxyhydroxides and P precipitated as Al- and Fe-P (see Table 3). An increase of NaOH-extractable P (representing Al- and Fe-associated P) with increasing soil age has also been observed in other tropical soils (Crews et al. 1995; Schlesinger et al. 1998), and is expected to occur significantly where ecosystems favor a formation of highly weathered soils such as in the central Amazon. In contrast, Al- and Fe-associated P constituted low proportions of total P in Pakistan's calcareous soils (ageing from <100 and 20,000 years; Ryan and Zghard 1979), in New Mexico desert soils (ageing from>3,000 and >25,000 years; Lajtha and Schlesinger 1988), and among eight USDA soil orders from all regions of the US (Tiessen et al. 1984).

Another major change in P forms was the increase in P_o fraction, which continued to increase beyond the period of dissolution of biogenic Ca-P and was dominant in the forest soil. This complemented mostly the Walker and Syers

(1976) model and findings in other tropical soils such as in Hawaii (Crews et al. 1995) and Indonesia (Schlesinger et al. 1998; Lawrence and Schlesinger 2001), and in temperate rain forest soils of New Zealand (Parfitt et al. 2005). The Hawaiian soils, however, exhibited a decrease in P_o from 150,000 to 4.1 million years following the increase that was also seen at our sites. Although its age is not precisely known, the P_o pool in the forest soil in our study was expected to show a declining trend. It is likely that during the 7,700 years of the Anthrosol studied, P_o has not reached its maximum, which was shown to exceed 150,000 years in the Hawaiian example (Crews et al. 1995).

Organic P plays an important role in defining long-term P bioavailability (Wardle et al. 2004), which depends on physical, chemical, and biological properties of soil during pedogenesis. Of the P_o species detected in New Zealand top soils under native vegetation (forest or scrub) by ^{31}P nuclear magnetic resonance (NMR) spectroscopy, both orthophosphate and orthophosphate monoesters initially increased in young soils (16,000 years old) and then declined in the oldest soils (130,000 years old) with time (McDowell et al. 2007). Concomitantly, labile P species (diesters and pyrophosphate) proportionally increased suggesting continued P cycling in the labile P_o fraction and in the microbial biomass. The authors suggested that the P_o cycling was still very active in soil at least for 130,000 years. The high P availability as a proportion of total P may in part be explained by a likely active cycling of P_o even after Ca-P disappeared in our study.

According to Syers and Walker (1969), both C/P_o and N/P_o ratios should decline during the aggrading phase (characterized by organic matter accumulation over time up to 500 years) as C and N accumulation rates slow more than P_o accumulation rate, then increase during the degrading or climax phase of the sequence (data available up to 10,000 years) as C and N retain longer than P_o in the system. The Anthrosols in the central Amazon showed the same trend being in the degrading system; both C/P_o and N/P_o ratios of the Anthrosols studied increased over time reaching to the climax of the system represented by the adjacent soil studies. This trend is in accordance with those in other ecosystems reviewed by McGill and Cole (1981).

Following the Walker and Syers (1976) model, occluded P_i increases during pedogenesis and becomes predominant with increasing time. Although occluded P_i increased until 2,150 years in the Anthrosols studied, it decreased thereafter and was only 17% of total P in the forest soil, which was a smaller fraction than in either adsorbed P_i and P_o fractions. To a certain degree, this can be explained by differences in soil texture and mineralogy between sites representing different times as mentioned above. However, occluded P_i was even dominant compared to other fractions in all adjacent Oxisols and Spodosol (45–70%). Inorganic P adsorbed on the metal surfaces of Al- and Fe-oxyhydroxides is known to experience an "ageing" effect becoming more difficult to desorb from the mineral surfaces over time (Martin et al. 2002). Mechanisms of this ageing of adsorbed P_i includes diffusion into microsites on oxide surfaces (interparticle diffusion), into the interior of oxide particles (intraparticle diffusion; Bolan et al. 1985), and transformation to stronger bonding between P and the oxide surfaces (inner-sphere complexation; i.e., from monodentate to bidentate complexes; Arai and Sparks 2001). It is neither possible nor one of the objectives to determine the ageing mechanism of P sorption in our study, and therefore further investigations are encouraged.

Nevertheless, the results from the P fractionation and the LCF analysis of XANES spectra on the Anthrosols studied generally agreed on the transformation of P in soil during pedogenesis on a long time scale. While the fractionation results only showed the exhaustion of Ca-bound P_i in the first ca. 2,000 years, the LCF results illustrated the transition of more stable Ca-P species (HAP) into more soluble species (TCP) and eventual exhaustion of both species within the same time scale. The presence of ACP1 (17%) in the DS sample is doubtful since its spectral quality was poor and the particular shoulder at 2,151–2,152 eV could not be unambiguously interpreted as either a spectral noise or a Ca-P feature (see Fig. 5a). The fractionation results showed, as the Ca-P disappeared, that the adsorbed P_i fraction increased to almost one half of the total P in the DS Anthrosol, which the LCF analysis could partially explain by the increase of the STR proportion which could represent the combined proportions of P adsorbed on Fe-oxyhydroxides and crystalline STR. However, while the LCF analysis showed the relatively constant and high proportion of Aq-PO_4 (58–65% of the total P) across the time scale studied, the fractionation results showed that the combined proportions of freely exchangeable P_i and P_o had a relatively small fraction (10–33% of the total P) with an increasing trend with increasing age of the Anthrosols.

5 Conclusions

Long-term transformation of biogenic Ca-P revealed overall consistent results with the Walker and Syers model for geogenic Ca-P transformation during pedogenesis. It appears that biogenic Ca-P (as CAP mostly derived from fish residues) deposited to soil transformed into more soluble Ca-P such as TCP at later stages. However, the rate of disappearance of biogenic Ca-P was ten times faster than that reported for geogenic Ca-P even at tropical sites. Phosphorus released from Ca-P was effectively adsorbed to Al- and Fe-oxyhydroxides, transformed into organic form, and/or converted to occluded fraction by 2,150 years of soil

formation. This concurs with observations of long-term transformation of geogenic Ca-P with P limitation developing over time (Vitousek and Farrington 1997). Compared to inorganic P sources, the studied biogenic Ca-P showed a comparatively long persistence and significantly increased P bioavailability for several hundred to a few thousand years. These results encourage further studies on the dissolution of biogenic Ca-P in soils and their interactions with mineral surfaces over shorter periods of time.

Acknowledgements The authors acknowledge NSF-DEB for funding under project number DEB-0425995. Any opinions, findings, and conclusions or recommendations expressed in this material are those of the authors and do not necessarily reflect the views of the NSF. We are thankful to Dr. Dean Hesterberg (Department of Soil Science, North Carolina State University) for providing spectral data for several aqueous phosphate species and valuable instruction and assistance for the LCF procedure of the XANES spectra. The authors also thank Dr. W. Caliebe for invaluable assistance with the spectroscopic analyses, performed at the beamline X-19A of the National Synchrotron Light Source, Project No. 4738. The NSLS is supported by the US Department of Energy under the contract No. DE-AC02-76CH00016.

References

Arai Y, Sparks DL (2001) ATR-FTIR spectroscopic investigation on phosphate adsorption mechanisms at the ferrihydrite-water interface. J Colloid Interface Sci 241:317–326

Beauchemin S, Hesterberg D, Chou J, Beauchemin M, Simard RR, Sayers DE (2003) Speciation of phosphorus in phosphorus-enriched agricultural soils using X-ray absorption near-edge structure spectroscopy and chemical fractionation. J Environ Qual 32:1809–1819

Bolan NS, Barrow NJ, Posner AM (1985) Describing the effect of time on sorption of phosphate by iron and aluminum hydroxides. Eur J Soil Sci 36:187–197

Chien SH, Menon RG (1995) Factors affecting the agronomic effectiveness of phosphate rock for direct application. Fert Res 41:227–234

Crews TE, Kitayama K, Fownes JH, Riley RH, Herbert DA, Mueller-Dombois D, Vitousek PM (1995) Changes in soil phosphorus fractions and ecosystem dynamics across a long chronosequence in Hawaii. Ecology 76:1407–1424

Cross AF, Schlesinger WH (1995) A literature review and evaluation of the Hedley fractionation: applications to the biogeochemical cycle of soil phosphorus in natural ecosystems. Geoderma 64:197–214

Gee GW, Or D (2002) Particle-size analysis. In: Dane JH, Topp GC (eds) Methods of soil analysis, Part 4, Physical Methods. Soil Sci Soc Am, Madison, Wisconsin, USA, pp 255–293

Hedin LO, Vitousek PM, Matson PA (2003) Nutrient losses over four million years of tropical forest development. Ecology 84:2231–2255

Holford ICR (1997) Soil phosphorus: its measurement, and its uptake by plants. Aust J Soil Res 35:227–239

Hsu PH (1977) Aluminum oxides and oxyhydroxides. In: Dixon JB, Weed SB (eds) Minerals in soil environments. Soil Sci Soc Am, Madison. Wisconsin, USA, pp 99–144

Hutchison KJ, Hesterberg D, Chou JW (2001) Stability of reduced organic sulfur in humic acid as affected by aeration and pH. Soil Sci Soc Am J 65:704–709

Kern DC, D'Aquino G, Rodrigues TE, Frazão FJL, Sombroek W, Myers TP, Neves EG (2003) Distribution of Amazonian Dark Earths in the Brazilian Amazon. In: Lehmann J (ed) Amazonian Dark Earths: origin, properties and management. Kluwer Academic, Dordrecht, pp 51–75

Lajtha K, Schlesinger WH (1988) The biogeochemistry of phosphorus cycling and phosphorus availability along a desert soil chronosequence. Ecology 69:24–39

Lawrence D, Schlesinger WH (2001) Changes in soil phosphorus during 200 years of shifting cultivation in Indonesia. Ecology 82:2769–2780

Lehmann J, da Silva CM, Zech W (2001) Organic matter stabilization in a Xanthic Ferralsol of the central Amazon as affected by single trees: chemical characterization of density, aggregate, and particle size fractions. Geoderma 99:147–168

Lehmann J, Campos CV, de Macêdo JLV, German L (2004) Sequential P fractionation of relic Anthropogenic Dark Earths of Amazonia. In: Glaser B, Woods WL (eds) Amazonian Dark Earths: explorations in space and time. Springer, Berlin, pp 113–123

Liang B, Lehmann J, Solomon D, Kinyangi J, Grossman J, O'Neill B, Sklemstad JO, Thies J, Luizão FJ, Petersen J, Neves EG (2006) Black carbon increases cation exchange capacity in soils. Soil Sci Soc Am J 70:1719–1730

Lima HN, Schaefer CER, Mello JWV, Gilkes RJ, Ker JC (2002) Pedogenesis and pre-Colombian land use of "Terra Preta Anthrosols" ("Indian black earth") of Western Amazonia. Geoderma 110:1–17

Lindsay WL, Vlek PLG, Chien SH (1989) Phosphate minerals. In: Dixon JB, Weed SB (eds) Minerals in soil environments, 2nd ed. Soil Sci Soc Am, Madison, Wisconsin, USA, pp 1089–1130

Martin M, Celi L, Barberis E (2002) Extractability and plant availability of phosphate from P-goethite complexes. Commun Soil Sci Plant Anal 33:143–153

McDowell RW, Cade-Menun B, Stewart I (2007) Organic phosphorus speciation and pedogenesis: analysis by solution ^{31}P nuclear magnetic resonance spectroscopy. Eur J Soil Sci 58:1348–1357

McGill WB, Cole CV (1981) Comparative aspects of cycling of organic C, N, S and P through soil organic matter. Geoderma 26:267–286

Murphy J, Riley JP (1962) A modified single solution method for the determination of phosphate in natural waters. Anal Chim Acta 27:31–36

Neves EG, Petersen JB, Bartone RN, Silva CAD (2003) Historical and socio-cultural origins of Amazonian Dark Earths. In: Lehmann J (ed) Amazonian Dark Earths: origin, properties and management. Kluwer Academic, Dordrecht, pp 29–50

Parfitt RL, Ross DJ, Coomes DA, Richardson SJ, Smale MC, Dahlgren RA (2005) N and P in New Zealand soil chronosequences and relationships with foliar N and P. Biogeochemistry 75:305–328

Pattan JN, Rao CM, Higgs NC, Colley S, Parthiban G (1995) Distribution of major, trace and rare-earth elements in surface sediments of the Wharton Basin, Indian Ocean. Chem Geol 121:201–215

Peak D, Sims JT, Sparks DL (2002) Solid-state speciation of natural and alum-amended poultry litter using XANES spectroscopy. Environ Sci Technol 36:4253–4261

Rao VP, Naqvi SW, Kumar MD, Cardinal D, Michard A, Borole DV, Jacobs E, Natarajan R (2000) A comparative study of Pleistocene phosphorites from the continental slope off western India. Sedimentology 47:945–960

Ryan J, Zghard MA (1979) Phosphorus transformations with age in a calcareous soil chronosequence. Soil Sci Soc Am J 44:168–169

Sale PWG, Mokwunye AU (1993) Use of phosphate rocks in the tropics. Fertil Res 35:33–45

Sato S, Solomon D, Hyland C, Ketterings QM, Lehmann J (2005) Phosphorus speciation in manure and manure-amended soils using XANES spectroscopy. Environ Sci Technol 39:7485–7491

Schaefer CEG, Lima HN, Gilkes RJ, Mello JWV (2004) Micromorphology and electron microprobe analysis of phosphorus and potassium forms of an Indian Black Earth (IBE) Anthrosol from Western Amazonia. Aust J Soil Res 42:401–409

Schlesinger WH, Bruijnzeel LA, Bush MB, Klein EM, Mace KA, Raikes JA, Whittaker RJ (1998) The biogeochemistry of phosphorus after the first century of soil development on Rakata Island, Kraakatau, Indonesia. Biogeochemistry 40:37–55

Sims JT, Pierzynski GM (2005) Chemistry of phosphorus in soils. In: Tabatabai MA, Sparks DL (eds) Chemical processes in soils. Soil Sci Soc Am, Madison, Wisconsin, USA, pp 151–192

Singleton GA, Lavkulich LM (1987) Phosphorus transformations in a soil chronosequence, Vancouver Island, British Columbia. Can J Soil Sci 67:787–793

Stevens PR, Walker TW (1970) The chronosequence concept and soil formation. Q Rev Biol 45:333–350

Syers JK, Walker TW (1969) Phosphorus transformations in a chronosequence of soils developed on wind-blown sand in New Zealand I. Total and organic phosphorus. J Soil Sci 20:57–64

Tang R, Hass M, Wu W, Gulde S, Nancollas GH (2003a) Constant composition dissolution of mixed phases II. Selective dissolution of calcium phosphates. J Colloid Interface Sci 260:379–384

Tang R, Henneman ZJ, Nancollas GH (2003b) Constant composition kinetics study of carbonated apatite dissolution. J Cryst Growth 239:614–624

Tarawneh K, Moumani K (2006) Petrography, chemistry and genesis of phosphorite concretions in the Eocene Umm Rijam Chert limestone Formation, Ma'an area, South Jordan. J Asian Earth Sci 26:627–635

Thomas RL, Sheard RW, Moyer JR (1967) Comparison of conventional and automated procedures for nitrogen, phosphorus and potassium analysis of plant material using a single digestion. Agron J 59:240–243

Tiessen H, Moir JO (1993) Characterization of available P by sequential extraction. In: Carter MR (ed) Soil sampling and methods of analysis. Can Soc Soil Sci. Lewis, Boca Raton, Florida, USA, pp 75–86

Tiessen H, Stewart JWB (1985) The biogeochemistry of soil phosphorus. In: Caldwell DE, Brierley JA, Brierley CL (eds) Planetary ecology. Van Nostrand Reinhold Company, New York, pp 463–472

Tiessen H, Stewart JW, Cole CV (1984) Pathways of phosphorus transformations in soils of differing pedogenesis. Soil Sci Soc Am J 48:853–858

USDA (1999) Soil taxonomy: a basic system of soil classification for making and interpreting soil surveys, 2nd edn. Natural Resources Conservation Service, USDA, Washington, DC, USA

USEPA (1983) Phosphorus, all forms, Method 365.1. In: Kopp JF, McKee GD (eds) Methods for chemical analysis of water and wastes, EPA-600/4-79-020. USEPA, Cincinnati, pp 365-1.1–365-1.7

USEPA (1995) Microwave assisted acid digestion of siliceous and organically based matrices. In: Test methods for evaluating solid waste, 3rd ed. USEPA, Washington, DC, USA, pp 3052-1-3052-20

Vitousek PM, Farrington H (1997) Nutrient limitation and soil development: experimental test of a biogeochemical theory. Biogeochemistry 37:63–75

Vitousek PM, Sanford RL (1986) Nutrient cycling in moist tropical forest. Annu Rev Ecol Syst 17:137–167

Vose RS, Schmoyer RL, Steurer PM, Peterson TC, Heim R, Karl TR, Eischeid J (1992) The global historical climatology network: long-term monthly temperature, precipitation, sea level pressure, and station pressure data. ORNL/CDIAC-53. Carbon Dioxide Inf. Anal. Cent., Oak Ridge Natl. Lab., Oak Ridge, Tennessee, USA

Walker TW, Syers JK (1976) The fate of phosphorus during pedogenesis. Geoderma 15:1–19

Wardle DA, Walker JR, Bardgett RD (2004) Ecosystem properties and forest declines in contrasting long-term chronosequences. Science 305:509–513